Polymer Journal (2018) 50:787–797
https://doi.org/10.1038/s41428-018-0055-5

ORIGINAL ARTICLE

Design and synthesis of PEGylated amphiphilic block oligomers as membrane anchors for stable binding to lipid bilayer membranes

Daiki Takahashi[1] · Yuta Koda[1,2] · Yoshihiro Sasaki[1] · Kazunari Akiyoshi[1,2]

Received: 31 January 2018 / Revised: 19 March 2018 / Accepted: 22 March 2018 / Published online: 7 May 2018

Abstract

Cell surface engineering is a potentially powerful method for manipulating living cells by decorating the cell membrane with specific molecules. Possible applications include cell therapy, drug delivery systems, bio-imaging, and tissue engineering. The stable binding of synthetic molecules to serve as artificial membrane protein anchors is a promising approach for appending functional molecules to the cell surface. However, such synthetic molecules have previously shown limitations, including cytotoxicity and low cell surface affinity. We synthesized amphiphilic block oligomers, using ruthenium-catalyzed living radical polymerization, as novel membrane anchors for stable binding to lipid bilayer membranes. AB and ABA-type amphiphilic block oligomers were synthesized with poly(ethylene glycol) methacrylate (PEGMA) and varying butyl methacrylate (BMA) contents (PEGMA/BMA ratios of 25/5–25/50). These PEGylated oligomers showed high binding efficiencies (up to 92%) for liposomes, which served as model cell membranes, and low cytotoxicity in K562 cells. Both the BMA content and the block segment sequence in the copolymers strongly affected their binding efficiencies. Oligomers with an ABA-type block structure were much more effective than AB-type block oligomers, random oligomers, or PEGMA homo-oligomers for stable membrane binding. Thus, precise control of the primary structures of the amphiphilic oligomers enabled tuning of their binding efficiencies. These amphiphilic block oligomers hold promise as novel membrane anchors in many biomedical applications.

Introduction

The cell membrane is regarded as an attractive thin-layer platform for manipulation in biological systems because it contains many functional molecules that are involved in, for example, signal transduction, material transport, and molecular recognition, and are condensed in the small space of a lipid bilayer membrane. On the cell surface, most such functional molecules are membrane proteins. With this background, cell surface engineering [1–3], a powerful tool to manipulate living cells by decorating the cell membrane with specific molecules, was developed to advance biomedical technology, including cell therapy, drug delivery systems, bio-imaging, and tissue engineering.

The stable binding of synthetic molecules to cell surfaces, to serve as artificial membrane proteins, is among the most promising approaches to appending functional molecules to the surfaces of cells or of liposomal model cells in cell surface engineering. For instance, synthetic receptors [4–6], membrane-anchored polymers for bone targeting [7], supramolecular ion channels [8], molecular engineered proteins to control cell–cell interactions [9, 10], and synthetic molecular transducers for transmembrane signal transduction [11, 12] have been described. However, few reports have described technologies for promoting the stable binding of synthetic molecules to the cell surface [13–15]. The limitations of developing such synthetic molecules include potential damage to cells by excess hydrophobic

Electronic supplementary material The online version of this article (https://doi.org/10.1038/s41428-018-0055-5) contains supplementary material, which is available to authorized users.

✉ Kazunari Akiyoshi
akiyoshi@bio.polym.kyoto-u.ac.jp
Yoshihiro Sasaki
sasaki@bio.polym.kyoto-u.ac.jp

[1] Department of Polymer Chemistry, Graduate School of Engineering, Kyoto University, Katsura, Nishikyo-ku, Kyoto 615-8510, Japan

[2] ERATO Akiyoshi Bio-Nanotransporter Project, Japan Science and Technology Agency (JST), Katsura Int'tech Center, Katsura, Nishikyo-ku, Kyoto 615-8530, Japan

moieties and decreased affinity to the hydrophilic cell membrane surface because of high hydrophobicity. Amphiphilic polymers and oligomers would be attractive candidates to address such concerns because their functions, as well as their hydrophobic properties for cell surface anchoring, can be readily designed using precision polymerization.

Recently, there has been increasing interest in living radical polymerization (LRP) [16–19] systems, which enable the easy preparation of functionalized macromolecules and oligomers as amphiphilic molecular materials. Hydrophilic and/or amphiphilic polymers obtained via an LRP system, such as poly[poly(ethylene glycol) methyl ether methacrylate] [poly(PEGMA)], poly(*N*-isopropylacrylamide), and their copolymers, are biocompatible and have been applied to protein stabilization [20–23] and patterning [24, 25] and as biocompatible carriers for drug delivery [26–29]. In particular, Sawamoto's LRP system with ruthenium catalysts (Ru-LRP) enables the synthesis of amphiphilic copolymers bearing many types of functional groups without any protecting groups [30–33]. The system enables the in situ preparation of amphiphilic block copolymers with high block efficiencies because of its high controllability, versatility, and functionality tolerance.

In this study, we synthesized PEGylated amphiphilic block co-oligomers as candidate membrane anchors for stable binding to cell membranes and investigated the effects of oligomer design on their binding efficiencies with liposomal lipid bilayer membranes [21], which we used as a model of the cell membrane (Fig. 1). AB-type diblock and ABA-type triblock oligomers were easily prepared with PEGMA and butyl methacrylate (BMA) via Ru-LRP. With the BMA content controlled, the resulting block oligomers bound efficiently to the membranes, with binding efficiencies much higher than those of corresponding random oligomers. In addition, ABA-type triblock oligomers bound more stably to the lipid membranes than did the AB-type diblock oligomers. Thus, precisely controlling the primary structure and hydrophobic content resulted in control of the binding efficiency of these block oligomers to lipid membranes. The PEGylated amphiphilic block oligomers obtained in this study would, therefore, be among the most promising membrane anchors, facilitating further

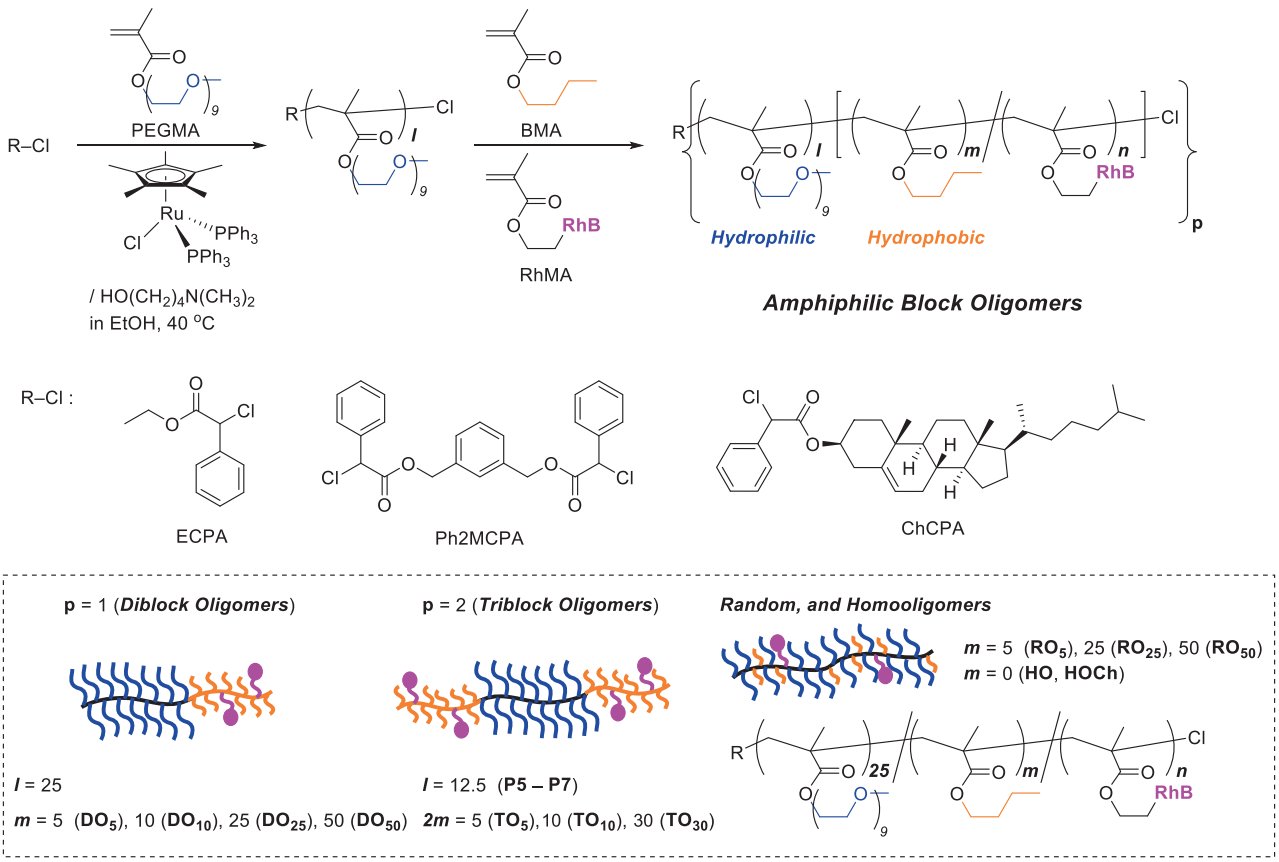

Fig. 1 Synthesis of amphiphilic oligomers via ruthenium-catalyzed living radical polymerization of poly(ethylene glycol) methyl ether methacrylate (PEGMA) and butyl methacrylate (BMA)

development of biomedical applications, including tissue and cell surface engineering.

Materials and methods/experimental procedures

Materials for the synthesis of initiators and monomers

2-Hydroxyethyl methacrylate (HEMA; TCI, Tokyo, purity >95%) was purged with nitrogen before use. Rhodamine B (RhB; Sigma-Aldrich, purity >95%), 4-dimethylaminopyridine (DMAP; TCI, purity ~99.0%), 1-(3-dimethylaminopropyl)-3-ethylcarbodiimide hydrochloride (EDC; TCI, purity >98.0%), triethylamine (Et_3N; TCI, purity >95.0%), α-chlorophenylacetyl chloride (CPAC; Sigma-Aldrich, purity >90%), cholesterol (Sigma-Aldrich, purity >99.0%), 1,3-benzene dimethanol (TCI, purity >98%), dichloromethane (Wako, super dehydrated for organic synthesis), chloroform (Wako, super dehydrated for organic synthesis, purity >99.0%), Wakogel® C-300 (Wako), hexane (Wako, purity >96%), ethyl acetate (Wako, purity >99.5%), chloroform (Wako, purity >99.0%), methanol (Wako, purity >99.8%), sodium chloride (Wako, purity >99.5%), sodium hydrogen carbonate ($NaHCO_3$; Wako, purity >99.5%), and sodium sulfate (Na_2SO_4; Wako, purity >99.0%) were used as received. H_2O was generated by a PURELAB Ultra Genetic (ELGA).

Materials for oligomer synthesis

Ethyl-2-chloro-2-phenylacetate (ECPA; Sigma-Aldrich, purity >98%), poly(ethylene glycol) methyl ether methacrylate (PEGMA; $CH_2=C(CH_3)CO_2(CH_2CH_2O)_9CH_3$, Sigma-Aldrich, M_n ~500), BMA (TCI, purity >99.0%), 4-dimethylamino-1-butanol (4-DMAB; TCI, purity >98.0%), 1,2,3,4-tetrahydronaphthalene (tetralin; TCI, purity >98%), toluene (Wako, super dehydrated for organic synthesis, purity ~99.5%), and ethanol (Wako, super dehydrated for organic synthesis, purity >99.5%) were dried over Na_2SO_4 and purged with nitrogen before use. $RuCp^*Cl(PPh_3)_2$ (Sigma-Aldrich, Cp*: pentamethylcyclopentadienyl) and SilliaBond metal scavenger (SilliaBond DMT; SilliCycle Inc.) were used as received.

Materials for liposomes

1,2-Dioleoyl-sn-glycero-3-phosphocholine (DOPC; Avanti Polar Lipids, 1 mg/mL >99.0%) in chloroform and 1,2-dioleoyl-sn-glycero-3-phosphoethanolamine-*N*-(7-nitro-2-1,3-benzoxadiazol-4-yl) ammonium salt (NBD–DOPE; Avanti Polar Lipids, 1 mg/mL >99.0%) were used as received. D-(−)-fructose (TCI, purity >99.0%), chloroform (Wako, super dehydrated for organic synthesis, purity >99.0%), methanol (Wako, super dehydrated for organic synthesis, purity ~99.8%), and 4-(2-hydroxyethyl)-1-piperazineethanesulfonic acid (HEPES, Nacalai Tesque) were used as received. Silica nanoparticles (Corefront, size = 5 μm, 50 mg/mL in water) were also used as received.

Characterization

The molecular weight distribution (MWD) curves, number average molecular weight (M_n), and dispersity (M_w/M_n) of the products were measured by size-exclusion chromatography (SEC) in THF at 40 °C (flow rate = 0.35 mL/min) on three linear-type polystyrene gel columns (TOSHO TSKgel Super-MultiporeHZ-H: exclusion limit = 4×10^7 g/mol; particle size = 6 μm; pore size = N/A; 4.6 mm i.d. × 15 cm) that were placed in an HLC-8320GPC (TOSHO) instrument equipped with refractive index and ultraviolet–visible detectors (wavelength = 254 nm). The columns were calibrated against 12 poly (methyl methacrylate) standards (Fluka; M_p = 800–1,600,000 g/mol; M_w/M_n = 1.02–1.14). ^1H and ^{13}C nuclear magnetic resonance (NMR) spectra were recorded in $CDCl_3$, CD_2Cl_2, DMSO-d_6, acetone-d_6, and D_2O at room temperature on a Bruker AscendTM 400 spectrometer operating at 400.13 (^1H) and 100.62 (^{13}C) MHz. Electrospray ionization–mass spectrometry (ESI–MS) analysis was performed on a mass spectrometer (Thermo Fisher Scientific). Dynamic light scattering (DLS) measurements were conducted on a Zetasizer Nano ZSP (Malvern) equipped with a He–Ne laser (λ = 633 nm) at 25 °C ([oligomer] = 10 mg/mL in HEPES/KOH buffer, pH ~7.5, 25 °C). The measuring angle was 173°, and the data were analyzed by the CUMULANT method. Transmission electron microscopy (TEM) measurements of oligomers were performed on an HT7700 (Hitachi) at an accelerating voltage of 100 kV. Samples were prepared by drop casting HEPES solutions of the oligomers (10 mg/mL) on carbon-coated grids (OKENSHOJI; ELS-C10 STEM Cu100P) and were stained with the vapor of a 1% aqueous OsO_4 solution. Confocal laser scanning microscopy (CLSM) measurements of liposomes were performed on a Zeiss LSM 780 (λ = 561 nm) at room temperature. To determine the binding efficiencies of the oligomers to liposomes, the fluorescence intensity (λ = 540 nm) was measured with a JASCO FP-8500 instrument at room temperature.

Synthesis of initiators and monomer

Synthesis of bifunctional chlorine-capped radical initiator (Ph2MCPA)

1,3-Benzene dimethanol (4.63 g, 33.5 mmol) was placed in a 300 mL round-bottomed flask, degassed, and equilibrated with argon. Dry CH_2Cl_2 (160 mL) and Et_3N (11.1 mL, 74.3

mmol) were added to the flask. CPAC (14.0 mL, 74.3 mmol) was slowly added to the solution at 0 °C (in an ice bath), and the mixture was stirred at room temperature overnight. After adding water to quench the reaction, the mixture was washed three times with saturated aqueous $NaHCO_3$ and once with brine, and the CH_2Cl_2 solution was dried over Na_2SO_4. After the removal of CH_2Cl_2 under vacuum, the crude product was purified by silica gel column chromatography with hexane/ethyl acetate (1/1, v/v) as the eluent. Evaporation of the eluent left a yellow oil. Yield: 14.8 g (66%). ^{1}H NMR (400 MHz, acetone-d_6, r.t., $\delta = 2.05$ (acetone)) δ 7.57–7.21 (m, 14 H, aromatic), 5.76 (s, 2 H), 5.21 (s, 4 H). ^{13}C NMR (100 MHz, acetone-d_6, r.t., $\delta =$ 206.26 (acetone)) δ 167.75 (C), 136.37 (C), 136.02 (C), 129.22–127.26 (CH, aromatic), 67.06 (CH_2), 58.79 (CH). ESI–MS: 465.06 *m/z* (found, M + Na), 443.32 *m/z* (calculated, M).

Synthesis of cholesteryl chlorine-capped radical initiator (ChCPA)

Cholesterol (11.9 g, 30.8 mmol) was placed in a 300 mL round-bottomed flask, degassed and equilibrated with argon. Dry CH_2Cl_2 (150 mL) and Et_3N (4.9 mL, 35 mmol) were added to the flask. CPAC (6.2 mL, 35 mmol) was slowly added to the solution at 0 °C (in an ice bath), and the mixture was stirred overnight at room temperature. After adding water to quench the reaction, the mixture was washed three times with saturated aqueous $NaHCO_3$ and once with brine, and the CH_2Cl_2 solution was dried over Na_2SO_4. After the removal of CH_2Cl_2 under vacuum, the crude product was purified by silica gel column chromatography with hexane/ethyl acetate (5/1, v/v) as the eluent. Evaporation of the eluent left a white solid, yield, 10.7 g (64%). ^{1}H NMR (400 MHz, $CDCl_3$, r.t., $\delta =$ 7.26 (chloroform)) δ 7.58–7.43 (m, 5 H, aromatic), 5.41–5.36 (dm, $J = 15.8$ Hz, 1 H), 5.34 (s, 1 H), 4.70 (m, 1 H), 2.38 (d, $J = 7.6$ Hz, 1 H), 2.27 (d, $J = 7.6$ Hz, 1 H), 2.03 (dm, $J = 12.5$, 1 H), 1.99–1.93 (m, 1 H), 1.91 (m, 1 H), 1.87 (m, 1 H), 1.83 (m, 1 H), 1.67–1.55 (m, 3 H), 1.54 (m, 1 H), 1.53–1.49 (m, 2 H), 1.49–1.46 (m, 1 H), 1.29 (m, 3 H), 1.22–1.11 (m, 6 H), 1.10 (m, 1 H), 1.08 (m, 1 H), 1.02 (m, 5 H), 0.90 (d, $J = 2.0$ Hz, 3 H), 0.88 (d, $J = 2.0$ Hz, 3 H), 0.69 (br s, 3 H). ^{13}C NMR (100 MHz, $CDCl_3$, r.t., $\delta = 77.16$ (chloroform)) δ 167.90 (C), 139.31 (CH), 136.18 (C), 129.32 (CH), 128.95 (CH), 128.06 (CH), 129.10 (CH), 123.23 (CH), 59.47 (C), 56.82 (CH), 56.28 (CH), 50.12 (CH), 42.46 (C), 39.85 (CH_2), 39.67 (CH_2), 37.91 (CH_2), 37.01 (CH_2), 36.70 (C), 36.33 (CH_2), 35.94 (CH_2), 31.98 (CH), 28.37 (CH_2), 28.16 (CH), 27.58 (CH_2), 24.42 (CH_2), 23.98 (CH_2), 22.97 (CH_3), 22.81 (CH_3), 21.18 (CH_2), 19.44 (CH_3), 18.87 (CH_3),12.00 (CH_3). ESI–MS: 561.35 *m/z* (found, M + Na), 1099.70 *m/z* (found, 2 M + Na), 1640.06 *m/z* (found, 3 M + Na), 538.36 *m/z* (calculated, M).

Synthesis of methacrylate monomer labeled with rhodamine B (RhMA)

RhB (13.1 g, 27.3 mmol) was placed in a 1000 mL three-neck round-bottomed flask, degassed, and equilibrated with argon. Dry chloroform (360 mL), HEMA (5.0 mL, 41 mmol), DMAP (836 mg, 6.80 mmol), and EDC (12.0 mL, 68.4 mmol) were added sequentially to the flask under argon flow. The reaction mixture was stirred overnight at room temperature. The mixture was then washed three times with brine, and the chloroform solution was dried over Na_2SO_4. After the removal of chloroform under vacuum, the crude product was semi-purified by silica gel chromatography with hexane/ethyl acetate (1/1, v/v) and chloroform/MeOH (5/1, v/v) as the eluents. The crude product was further purified by silica gel column chromatography with chloroform/MeOH (25/1, v/v) and MeOH as the eluents. The evaporation of the eluents left a dark purple oil, yield, 16.2 g (41%). ^{1}H NMR (400 MHz, $CDCl_3$, r.t., $\delta = 7.26$ (chloroform)) δ 8.31 (d, $J = 7.34$ Hz, 1 H), 7.89–7.65 (m, 3 H), 7.06–7.12 (m, 1 H), 6.92–6.97 (m, 1 H), 6.70–6.82 (m, 1 H), 6.05 (s, 1 H), 5.58 (s, 1 H), 4.33 (m, 2 H), 4.21 (m, 2 H), 4.14–3.60 (m, 4 H), 3.60 (m, 4 H), 1.92 (s, 3 H), 1.28 (m, 6 H), 1.11 (t, $J = 7.09$ Hz, 6 H). ^{13}C NMR (100 MHz, $CDCl_3$, r.t., $\delta = 77.16$ (chloroform)) δ 169.36 (C), 162.00 (C), 157.70 (C), 155.52 (C), 154.10 (C), 150.53 (C), 136.21 (C), 135.30 (C), 133.84 (C), 131.42 (CH), 131.21 (CH), 130.46 (CH), 129.37 (C), 126.08 (CH), 125.87 (CH), 125.00 (CH_2), 114.12 (CH), 108.99 (CH), 107.24 (C), 97.24 (CH), 96.30 (CH), 18.32 (CH_3), 13.72 (CH_3). ESI–MS: 556.26 *m/z* (found, M + H), 555.25 m/z (calculated, M).

Oligomer synthesis

The synthesis of the oligomers was performed by a syringe technique under argon in glass tubes equipped with a three-way stopcock, using Ru-LRP. Typical procedures were as follows: **DO_{25}** (PEGMA/BMA diblock co-oligomer): $RuCp^*Cl(PPh_3)_2$ (60 mg, 0.076 mmol) was solubilized with toluene (2.0 mL) in a 100 mL round-bottomed flask. EtOH (26 mL), tetralin (0.9 mL), 4-DMAB (0.2 mL, 1.6 mmol), PEGMA (8.7 mL, 19 mmol), and ECPA (0.13 mL, 0.76 mmol) were added sequentially to the flask at 0 °C (in an ice bath) under an argon flow (total volume: 37.8 mL). An aliquot of the mixture (8.0 mL) was transferred to a glass tube and maintained at 40°C in an oil bath. After 49 h (89% conversion determined by ^{1}H NMR), oligo(PEGMA)–Cl was obtained (M_n (NMR) = 14,700 g/mol, M_w/M_n (SEC) = 1.16). Then, BMA (1.2 mL, 7.9 mmol), 4-DMAB (0.06 mL,

0.48 mmol), and 336 mM RhMA (1.2 mL, 0.40 mmol) in EtOH were directly added to the oligo(PEGMA)–Cl solution at 0 °C (ice bath) under argon flow without any purification, and the glass tube was then placed again in an oil bath (40 °C). After 9 h, the conversion of BMA had reached 49%, as determined by ^{1}H NMR, and the polymerization was quenched by cooling to −196 °C in liquid N_2. The crude product was semi-purified using SilliaBond DMT (0.5 g) and dialyzed against methanol/water (9/1, v/v) in a regenerated cellulose membrane (Spectra/Por® 7; molecular weight cut-off (MWCO) 2000). The inner aqueous solution was lyophilized to yield a purple solid product (**DO$_{25}$**). SEC (THF, PMMA std.): M_n (SEC) = 11,600 g/mol; M_w/M_n (SEC) = 1.16 (Figure S2). ^{1}H NMR (400 MHz, CD_2Cl_2, r.t., $\delta = 5.32$ ($CHDCl_2$)): δ 7.4–7.2 (aromatic), 4.2–4.1 (–COOCH_2CH$_2$O–), 4.0–3.9 (–COOCH_2CH$_2$CH$_2$CH$_3$), 3.8–3.6 (–OCH_2CH_2O–), 3.6–3.5 (–OCH$_2$CH_2OCH$_3$), 3.4–3.3 (–OCH$_2$CH$_2$OCH_3), 2.1–1.4 (–CH$_2$–), 1.8 (–COOCH$_2$CH_2CH$_2$CH$_3$), 1.7–1.6 (–COOCH$_2$CH$_2$CH_2CH$_3$), 1.5–1.4 (–COOCH$_2$CH$_2$CH$_2$CH_3), 1.2–0.7 (–CCH$_3$). M_n (NMR) = 15,700 g/mol (*DP* (PEGMA) = 26, *DP* (BMA) = 19). Other PEGMA/BMA diblock co-oligomers (**DO$_5$**, **DO$_{10}$**, and **DO$_{50}$**) were synthesized with the same catalytic system as **DO$_{25}$** (Figure S2).

TO$_{10}$ (PEGMA/BMA triblock co-oligomer): RuCp*Cl(PPh$_3$)$_2$ (61 mg, 0.077 mmol) was dissolved in toluene (2.0 mL) in a 100 mL round-bottomed flask. EtOH (22 mL), tetralin (0.88 mL), a 411 mM EtOH solution of 4-DMAB (3.7 mL, 1.5 mmol), PEGMA (8.9 mL, 19.22 mmol), and an 811 mM DMF solution of Ph2MCPA (0.94 mL, 0.76 mmol) were added sequentially to the flask at 0 °C (in an ice bath) under an argon flow (total volume, 38.0 mL). An aliquot of the mixture (8.0 mL) was transferred to a glass tube and maintained at 40 °C with an oil bath. After 25 h (85% conversion, by ^{1}H NMR), oligo(PEGMA)–Cl was obtained (Figure S1a and b; M_n (NMR) = 10,600 g/mol, M_w/M_n (SEC) = 1.21). Then, BMA (0.51 mL, 3.19 mmol), a 410 mM EtOH solution of 4-DMAB (1.2 mL, 0.49 mmol) and a 336.2 mM EtOH solution of RhMA (1.2 mL, 0.40 mmol) were directly added to the oligo(PEGMA)–Cl solution at 0 °C (in an ice bath) under an argon flow without any purification, and the glass tube was again placed in an oil bath (40 °C). After 5 h, the conversion of BMA had reached 46%, as determined by ^{1}H NMR, and polymerization was quenched by cooling to −196 °C (liquid N_2) (Figure S1a). The crude product was semi-purified by SilliaBond DMT (0.5 g) and dialyzed against methanol/water (9/1, v/v) in a regenerated cellulose membrane (Spectra/Por® 7; MWCO 2000). The inner aqueous solution was lyophilized to yield a purple solid (**TO$_{10}$**). SEC (THF, PMMA std.): M_n (SEC) = 14,100 g/mol; M_w/M_n (SEC) = 1.28 (Figure S1b). ^{1}H NMR (400 MHz, CD_2Cl_2, r.t., $\delta = 5.32$ ($CHDCl_2$)): δ 7.4–6.9 (aromatic), 6.2, 5.6 (olefin), 4.2–4.1 (–COOCH_2CH$_2$O–), 4.0–3.9 (–COOCH_2CH$_2$CH$_2$CH$_3$), 3.8–3.6 (–OCH_2CH_2O–), 3.6–3.5 (–OCH$_2$CH_2OCH$_3$), 3.4–3.3 (–OCH$_2$CH$_2$OCH_3), 2.1–1.4 (–CH$_2$–), 1.8 (–COOCH$_2$CH_2CH$_2$CH$_3$), 1.7–1.6 (–COOCH$_2$CH$_2$CH_2CH$_3$), 1.5–1.4 (–COOCH$_2$CH$_2$CH$_2$CH_3), 1.2–0.8 (–CCH$_3$). M_n (NMR) = 18,000 g/mol (Figure S1c; *DP* (PEGMA) = 34, *DP* (BMA) = 5.5). Other PEGMA/BMA triblock oligomers (**TO$_5$** and **TO$_{30}$**) were synthesized with the same catalytic system as **TO$_{10}$** (Figure S2).

Cytotoxicity assay

K562 cells (JCRB Cell Bank) were cultured in RPMI containing 10% fetal bovine serum (FBS) and 1% penicillin–streptomycin at 37 °C in a humidified atmosphere of 95% air and 5% CO_2. For the WST-8/lactate dehydrogenase (LDH) assay, K562 cells (5.6×10^3 cells per mL) were collected by centrifugation. A phosphate-buffered saline (PBS) solution of an oligomer (10 µL; 0.10, 1.0, 10, or 100 µM), PBS (Thermo Fisher Scientific, 1×, 10 µL) as a negative control, or 0.2% Tween 20 (10 µL) as a positive control for the LDH assay was added to the cell solution (90 µL, 5.6×10^3 cells per mL) in a plate reader. The mixtures were incubated at 37 °C for 24 h in a humidified atmosphere of 95% air and 5% CO_2. For the WST-8 assay, CCK-8 (Cell Counting Kit-8, Dojindo) solution was added, and the mixtures were incubated at 37 °C in a humidified atmosphere with 95% air and 5% CO_2 for 3 h. After the incubation, the absorbance of each well at 450 nm was measured, using a reference wavelength of 650 nm. For the LDH assay, LDH solution was added to the supernatants from the cells, and the mixtures were incubated for 45 min at 37 °C in a humidified atmosphere with 95% air and 5% CO_2. After the incubation, aqueous HCl (10 µL, 1 mol/L) was added to the samples to stop the chromogenic reaction. The absorbance of each well at 562 nm was measured. The cytotoxicity and cell membrane damage were calculated from these absorbance values.

Characterization of oligomer binding to liposomes

Giant liposomes were prepared as follows: [34] DOPC (10 µL, 0.10 µmol, 10 mM), NBD–DOPE (0.1 mM, 5 µL, 0.0005 µmol), and fructose (150 mM, 16.6 µL, 2.49 µmol) were dissolved in chloroform (68.4 µL). The solvents were removed under an argon flow to form a thin lipid film on the glass tube. The thin film was dried overnight under reduced pressure. After HEPES/KOH buffer (10 mM, pH = 7.5, 100 µL) was added to the glass tube, the tube was incubated at 37 °C for 6 h to hydrate the lipid membranes. This procedure yielded a giant liposome suspension. A 1.0 mM methanol solution of the oligomer

(1 μL, 0.001 μmol) was added to the liposome solution (1 mM, 100 μL), and the mixture was examined by CLSM ($\lambda = 561$ nm).

Binding efficiency of oligomers to liposome/silica preparations

A 10 mM chloroform solution of DOPC (1.0 mL, 0.010 mmol) was placed in a 20 mL round-bottomed flask. The chloroform was removed under an argon flow to form a thin film on the glass tube. The flask was dried overnight under reduced pressure. After 10 mM HEPES/KOH buffer (1.0 mL, pH = 7.5) was added to the flask, the flask was placed at 37 °C for 4 h to hydrate the lipid membranes. The solution was then vortexed and then sonicated in a 0 °C bath with a probe-type sonicator (30 min, 60 W). After filtration through a 0.22 μm filter, a silica nanoparticle suspension in HEPES/KOH buffer (particle diameter = 5 μm, 50 mg/mL, 100 μL) was added to the liposome solution (10 mM, 500 μL). After stirring for 30 min, the clear supernatant was removed by centrifugation (1600×*g*, 5 min), and 10 mM HEPES/KOH buffer (500 μL) was added to the tube. This procedure yielded an aqueous liposome/silica (10 mg/mL) suspension.

A 1.0 mM methanol solution of oligomer (1.0 μL, 0.0010 μmol) was added to the liposome/silica solution (10 mg/mL, 50 μL). This mixture was centrifuged (1600×*g*, 5 min), and the fluorescence intensity of its clear supernatant was measured ($I_{\text{free oligomer}}$, $\lambda = 540$ nm). The fluorescence intensity of an original oligomer solution (I_{original}) was also measured to enable calculation of the binding efficiency of the oligomer to the lipid membranes by the following equation: $100 \times (1 - I_{\text{free oligomer}}/I_{\text{original}})$.

Results and discussion

Synthesis and characterization of amphiphilic oligomers

Amphiphilic block oligomers, as candidate membrane anchors, were prepared by Ru-LRP from PEGMA and BMA. AB-type and ABA-type block oligomers were synthesized, and the BMA content was varied to investigate the impact of each oligomer composition on its binding efficiency to lipid bilayer membranes. The following points were considered in designing oligomers as membrane anchors. (1) To solubilize the oligomers in water, PEG side chains, which have relatively low cytotoxicity, were grafted to the oligomers. (2) BMA segments were adopted as hydrophobic anchoring units, and their hydrophobicity was tuned by adjusting the BMA content to investigate the effects on their binding affinity to lipid membranes. (3) To investigate the primary structure of the oligomers, diblock and triblock oligomers were designed.

For synthesis of those block oligomers, PEGMA was polymerized with a chloride initiator (ethyl-2-chloro-2-phenylacetate, ECPA) and $RuCp^*Cl(PPh_3)_2$/4-DMAB (Cp*, pentamethylcyclopentadienyl; 4-DMAB, 4-(dimethylamino)-1-butanol) in ethanol at 40 °C (Fig. 1; $\boldsymbol{l}$ = PEGMA/ECPA = 25) [31, 32]. Up to 89% of the PEGMA was consumed to yield oligo(PEGMA)–Cl (M_n (SEC) = 9700, M_w/M_n (SEC) = 1.12), and BMA and methacrylate monomer labeled with rhodamine B (RhMA) were added in situ to the solution (BMA/oligo(PEGMA)–Cl = 10 (**DO_5**), 20 (**DO_{10}**), 50 (**DO_{25}**), 100 (**DO_{50}**); RhMA/oligo (PEGMA)–Cl = 2.5). We added a twofold excess of monomer in the second step to avoid obtaining oligomers bearing olefin terminal ends, which are potentially cytotoxic, and the degree of polymerization (DP) was targeted to $\boldsymbol{m}$ = BMA/ECPA = 5 (**DO_5**), 10 (**DO_{10}**), 25 (**DO_{25}**), 50 (**DO_{50}**), and $\boldsymbol{n}$ = RhMA/ECPA = 1.3. Indeed, the second polymerization was completely stopped at point when ~50% of the BMA was consumed. Each block oligomer was obtained at a narrow MWD (Table 1; M_n (SEC) = 11,600 – 21,300, M_w/M_n (SEC) = 1.09–1.18). Because of the solubility of the PEG side chains in CH_2Cl_2, the absolute number average molecular weight of those oligomers (M_n(NMR)) and the *DP* value for each monomer were determined by ^{1}H NMR in CD_2Cl_2 (Table 1; M_n (NMR) = 13,600–20,800; *DP* (PEGMA) = 25–36; *DP* (BMA) = 6–54). All M_n (NMR) and DP values corresponded closely to their respective target values. ABA-type triblock oligomers (**TO_5**–**TO_{30}**) were similarly synthesized with a bifunctional chlorine-capped radical initiator (Ph2MCPA, Fig. 1) using the same system. They were also obtained with high block efficiencies and narrow MWDs (Table 1; M_n (NMR) = 18,000–18,500 (**TO_5**–**TO_{30}**); M_w/M_n (SEC) = 1.15–1.28 (**TO_5**–**TO_{30}**); $\boldsymbol{l}$ = 12.5, $\boldsymbol{m}$ = 2.5 (**TO_5**), 5 (**TO_{10}**), and 15 (**TO_{30}**)). In the same way, random oligomers ($\boldsymbol{l}$ = 25, $\boldsymbol{m}$ = 5 (**RO_5**), 25 (**RO_{25}**), 50 (**RO_{50}**), $\boldsymbol{n}$ = 1.3) and PEGMA homo-oligomers (**HO** and **HOCh**; $\boldsymbol{l}$ = 25, $\boldsymbol{m}$ = 0, $\boldsymbol{n}$ = 1.3) were synthesized to compare their binding efficiencies to lipid membranes with those of **DO_5**–**DO_{50}** (Table 1; M_n (NMR) = 13,600–20,800, M_w/M_n (SEC) = 1.09–1.18).

These amphiphilic oligomers could be dispersed in water because the grafting of hydrophilic PEG side chains and hydrophobic BMA segments resulted in the formation of self-assembled structures in water. Indeed, their hydrodynamic radii (R_H values), determined by DLS, were 6.3 (**DO_{10}**), 10 (**DO_{25}**), 65 (**DO_{50}**), and 26 (**TO_{30}**) nm in HEPES [4-(2-hydroxyethyl)-1-piperazineethanesulfonic acid] buffer (Fig. 2a, b, Table S1; pH ~7.5, [oligomer] = 10 mg/mL, 25 °C). TEM analysis showed that **DO_{10}**–**DO_{50}** and **TO_{30}** formed spherical, probably micellar, structures (Fig. 2a, c;

Table 1 Characterization of PEGMA/BMA-based amphiphilic oligomers[a]

Code	Initiator	Structure	Time (h)	***l*/*m*/*n*/p**[b]	Conversion (%)[c] PEGMA/ BMA	M_n[d] (SEC)	M_w/M_n[d] (SEC)	***l*/*m*$_{obsd}$**[e] (NMR)	M_n[e] (NMR)
DO$_5$	ECPA	Diblock	59	25/5/1.3/1	88/65	13,700	1.09	25/6	13,600
DO$_{10}$	ECPA		54	25/10/1.3/1	85/50	13,400	1.18	36/11	19,700
DO$_{25}$	ECPA		58	25/25/1.3/1	96/49	11,600	1.16	26/19	15,700
DO$_{50}$	ECPA		69	25/50/2.5/1	86/50	21,300	1.12	26/54	20,800
TO$_5$	Ph2MCPA	Triblock	35	12.5/2.5/ 0.65/2	89/44	16,500	1.15	18/1.4	18,500
TO$_{10}$	Ph2MCPA		30	12.5/5/ 0.65/2	94/46	14,100	1.28	17/5.5	18,000
TO$_{30}$	Ph2MCPA		29	12.5/15/ 0.65/2	88/51	14,300	1.23	16/15	18,300
RO$_5$	ECPA	Random	57	25/5/2.5/1	95/100	15,700	1.12	38/5	20,000
RO$_{25}$	ECPA		51	25/25/2.5/1	87/93	25,600	1.09	26/29	17,600
RO$_{50}$	ECPA		57	25/50/2.5/1	85/89	20,900	1.23	30/55	22,900
HO	ECPA	Homo	56	25/0/2.5/1	92/—	17,700	1.07	36/—	18,300
HOCh	ChCPA		48	25/0/2.5/1	92/—	18,200	1.08	35/—	17,900

[a]**DO$_5$–DO$_{50}$**, **TO$_5$–TO$_{30}$**: $[PEGMA]_0/[Initiator]_0/[RuCp^*Cl(PPh_3)_2]_0/[4\text{-}DMAB]_0//[BMA]_{add}/[RhMA]_{add}/[4\text{-}DMAB]_{add}$ = 500/20/2.0/40/200, 400, 1000, 2000/50/60 mM in EtOH at 40 °C. **RO$_5$–RO$_{50}$**: $[PEGMA]_0/[BMA]_0/[RhMA]_0/[ECPA]_0/[RuCp^*Cl(PPh_3)_2]_0/[4\text{-}DMAB]_0$ = 500/5, 25, 50/50/20/2.0/40 mM in EtOH at 40 °C. **HO**, **HOCh**: $[PEGMA]_0/[RhMA]_0/[Initiator]_0/[RuCp^*Cl(PPh_3)_2]_0/[4\text{-}DMAB]_0$ = 500/50/20/2.0/40 mM in EtOH at 40 °C

[b]Calculated degrees of polymerization of PEGMA, BMA, and RhMA: $\boldsymbol{l} = [PEGMA]_0/[chlorine]_0$; $\boldsymbol{m} = [BMA]/[chlorine]_0$; $\boldsymbol{n} = [RhMA]/[[chlorine]_0$; **p** = 1 (monofunctional initiator; ECPA or ChCPA), 2 (bifunctional initiator; Ph2MCPA) (Fig. 1)

[c]Monomer conversion: determined by ^{1}H NMR

[d]Number average molecular weight (M_n) and molecular weight distribution (M_w/M_n): determined by size-exclusion chromatography (SEC) in THF with PMMA standards

[e]Observed ***l*** and ***m*** in oligomers and M_n, determined by ^{1}H NMR

D_{ave} = 22–85 nm). In contrast, the R_H values of **DO$_5$**, **TO$_5$**, and **TO$_{10}$** were much lower than those of **DO$_{10}$–DO$_{50}$** (Table S1; R_H = 2.7 (**DO$_5$**), 3.1 (**TO$_5$**), and 3.3 (**TO$_{10}$**) nm). Thus, **DO$_5$**, **TO$_5$**, and **TO$_{10}$** appeared to exist as unimers in water. Peaks from the BMA segment almost disappeared in ^{1}H NMR spectra conducted in D_2O, indicating that the semi-long PEG side chains of **DO$_5$**, **TO$_5$**, and **TO$_{10}$** were solubilized as unimers in water (Figure S1).

Cytotoxicity study

The cytotoxicity of the block oligomers, **DO$_5$**, **DO$_{25}$**, **TO$_{10}$**, **RO$_{25}$**, and **HO**, was evaluated in K562 cells. A HEPES buffer solution of each oligomer at various concentrations was added to K562 cell cultures (1.0 mL, [oligomer] = 0.01–10 μM, 5000 cells per mL), and the cells were cultured at 37 °C for 24 h. Cell proliferation and damage were measured using WST-8 [2-(2-methoxy-4-nitrophenyl)-3-(4-nitrophenyl)-5-(2,4-disulfophenyl)-2H tetrazolium, monosodium salt] and lactate dehydrogenase (LDH) assays, respectively (Fig. 3). In the WST-8 assay, the K562 cells maintained their normal rates of proliferation, even in the presence of the oligomers, with cell viabilities of 51–91% (**DO$_5$**), 83–86% (**DO$_{25}$**), 59–100% (**TO$_{10}$**), 74–84% (**RO$_{25}$**), and 75–88% (**HO**), (Fig. 3a). In addition, these co-oligomers hardly damaged the cell membranes (cell damage ~0.2–3.1% (**DO$_5$**), 0.1–5.3% (**DO$_{25}$**), 0–13.2% (**TO$_{10}$**), 2.9–6.6% (**RO$_{25}$**), and 0–5.7% (**HO**)), as determined by the LDH assay (Fig. 3b). Therefore, we concluded that these amphiphilic oligomers showed relatively low cytotoxicity in the range of concentrations tested.

PEGylated amphiphilic oligomers as membrane anchors

Amphiphilic oligomers were added to giant liposomes fluorescently labeled with NBD–DOPE (oligomer/DOPC/NBD–DOPE = 1/10/0.05, mol/mol/mol) to observe the interaction of oligomers with liposomes, the latter as a model of the cell membrane, by CLSM. Not only block oligomers but also random oligomers and homo-oligomers were attached to the membranes of the liposomes, as confirmed by the overlap of two-color fluorescence-labeled microscopic images showing rhodamine B on the oligomer

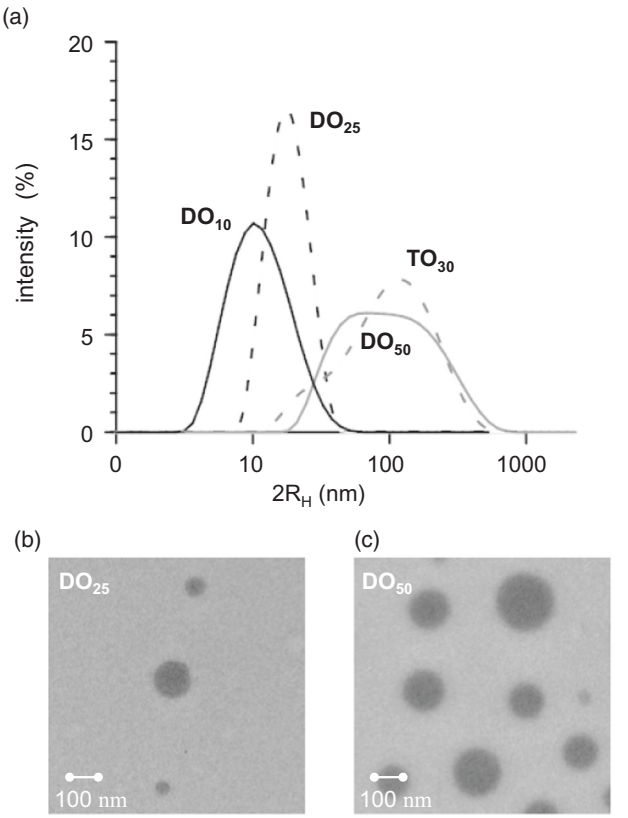

Fig. 2 DLS intensity distribution of (**a**) **DO_{10}–DO_{50}** and **TO_{30}** (black, **DO_{10}**; black dash, **DO_{25}**; gray, **DO_{50}**; gray dash, **TO_{30}**) in HEPES/KOH buffer solution at 25 °C ([oligomer] = 10 mg/mL, pH ~7.5). TEM images of (**b**) **DO_{25}** and (c) **DO_{50}** from HEPES/KOH solutions, cast on carbon grids and stained with OsO_4 ([oligomer] = 10 mg/mL, pH ~7.5)

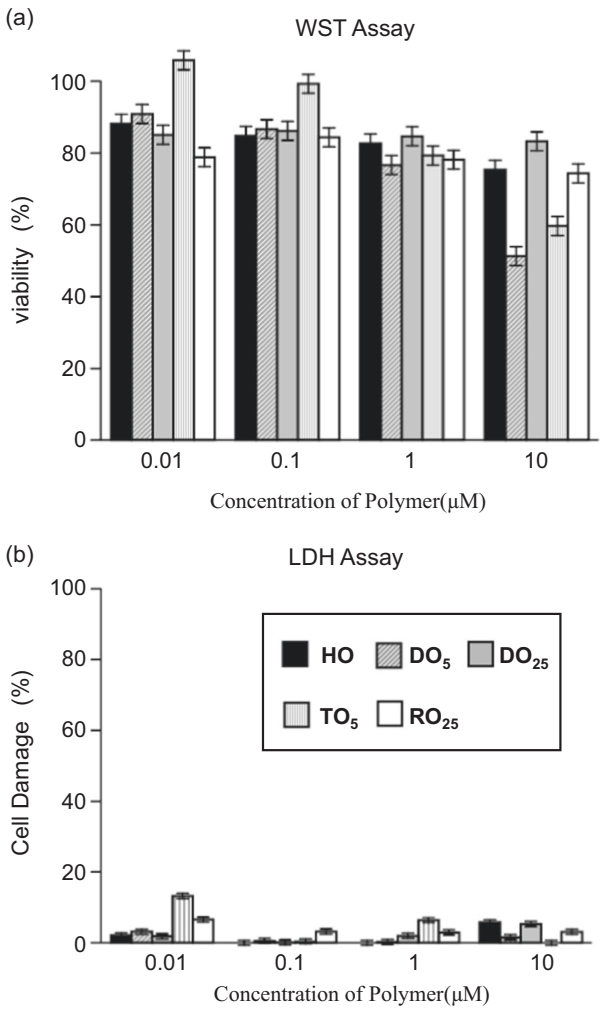

Fig. 3 K562 cell (**a**) viability and (**b**) damage in the presence of **DO_5** (gray and slash marks), **DO_{25}** (gray), **TO_{10}** (gray and vertical marks), **RO_{25}** (white) and **HO** (black), determined by (**a**) WST or (**b**) LDH assay; [oligomer] = 0.01, 0.1, 1.0, or 10 μM in PBS, pH = 7.4

and NBD on the phospholipid molecule (Figs. 4a, b and S4). These results indicated that the amphiphilic oligomers definitely interacted with lipid bilayer membranes, probably by primarily hydrophobic interactions.

The binding efficiencies of the oligomers with lipid bilayer membranes were quantified using hybrid liposomes with silica particles, which can be easily separated from free/unbound oligomers by mild centrifugation (Fig. 4c). The amphiphilic oligomers also bound to lipid bilayer membranes on silica particles, as they did to liposomes alone, as shown by fluorescence microscopy (Fig. 4d, e). A methanol solution of an oligomer (2.5 μL, 1.0 mM) was added to a suspension of lipid bilayer-coated silica particles (silica particle; 10 mg/mL, $[\text{oligomer}]_{\text{final}} = 12.5$ μM; oligomer/lipid = 1/10, mol/mol). After vortexing, the solution was centrifuged (1600×*g*, 5 min) to separate the lipid bilayer-coated silica particles from the solution containing unbound oligomers. The fluorescence intensity of the supernatant containing free oligomers was quantified by fluorescence spectrophotometry ($I_{\text{free oligomer}}$) and compared with that of the original solution (I_{original}; $[\text{oligomer}]_{\text{final}} =$ 12.5 μM) to determine the binding efficiency of the oligomer to the lipid bilayer-coated silica particles, as described in "Materials and methods/experimental procedures."

The binding efficiencies of the oligomers to the lipid bilayer membranes were 44% (**DO_5**), 16% (**DO_{10}**), 8.8% (**DO_{25}**), and 7.4% (**DO_{50}**), indicating that oligomer binding depended on the content of BMA as a hydrophobic segment (Fig. 5, Table S2). **DO_5**, which has the lowest BMA content in the series of **DO_n** oligomers, showed the most efficient binding to the lipid membranes, probably because of the higher affinity of unimeric **DO_5** to lipid bilayer membranes (Fig. 2a, b). The more hydrophobic oligomers (**DO_{10}–DO_{50}**), which formed micelles in water, showed lower efficiency, potentially because their self-assembled micellar forms were more stable than their lipid bilayer-bound states. In addition, the binding efficiencies of random oligomers (**RO_5–RO_{50}**) and PEGMA homo-oligomers (**HO**) were

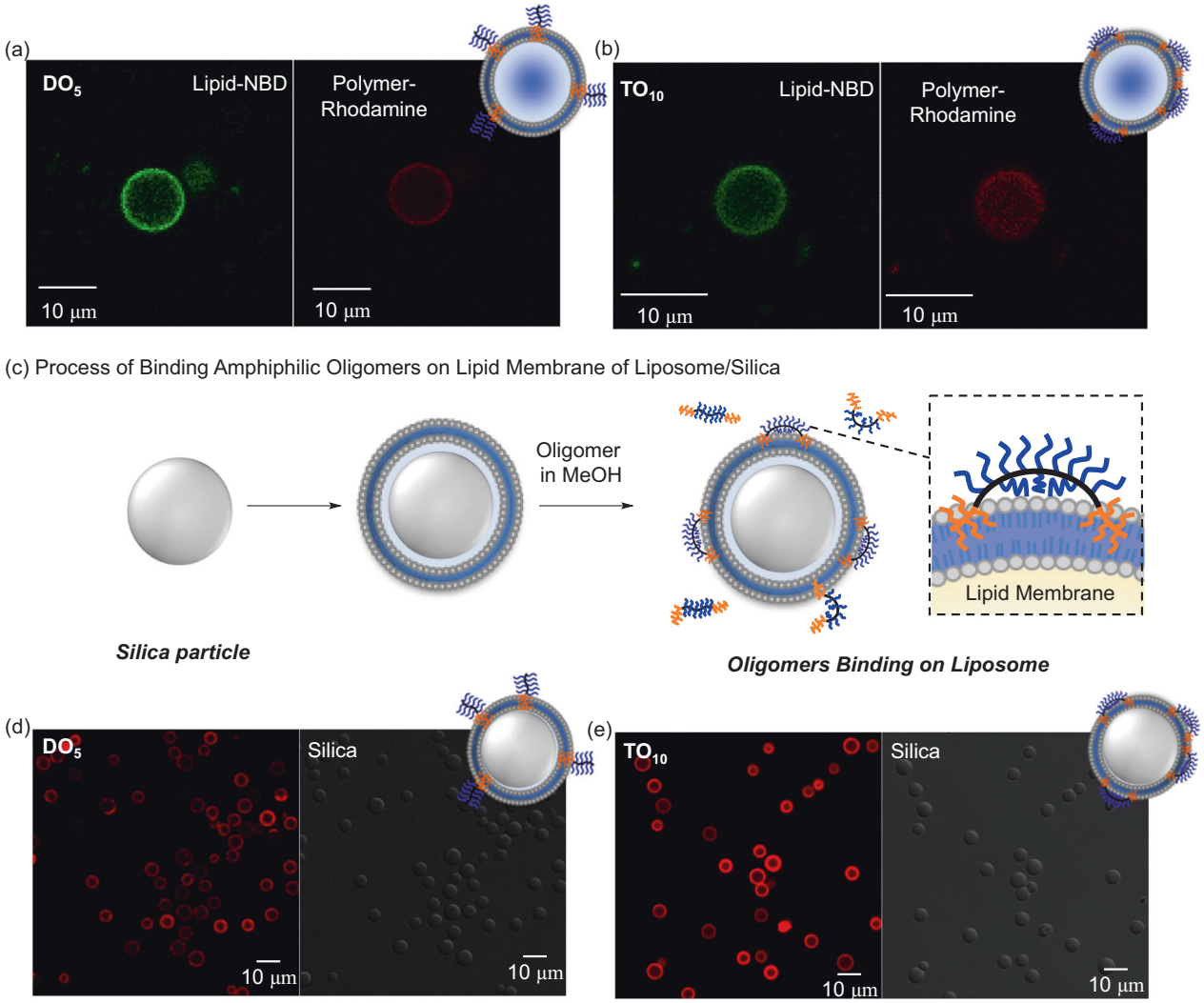

Fig. 4 CLSM images of liposomes with (**a**) $\mathbf{DO_5}$ and (**b**) $\mathbf{TO_{10}}$. The fluorescence of NBD and rhodamine were measured at 488 and 562 nm laser excitation, respectively. Conditions: [oligomer]/[DOPC]/[NBD–DOPE] = 1/10/0.05 (mol/mol/mol) in HEPES buffer/methanol = 100/1 (v/v) at 25 °C. **c** Experimental process of binding amphiphilic oligomers on lipid membranes of liposome/silica in HEPES buffer solution. CLSM images of liposome/silica with (**d**) $\mathbf{DO_5}$ and (**e**) $\mathbf{TO_{10}}$. Conditions: [oligomer]/[DOPC] = 1/10 (mol/mol) in HEPES buffer/methanol = 100/1 (v/v) at 25 °C

determined to compare them to that of $\mathbf{DO_5}$. The efficiencies were 29% ($\mathbf{RO_5}$), 17% ($\mathbf{RO_{25}}$), 8.2% ($\mathbf{RO_{50}}$), 28% (**HO**), and 28% (**HOCh**) (Table S2). These results indicated that not only BMA content but also the block segment sequence of the copolymer affected its binding affinity to the lipid membranes (Fig. 5). A homo-oligomer made hydrophobic with cholesterol at the end groups did not show increased binding affinity.

The binding efficiencies of ABA-type triblock oligomers ($\mathbf{TO_5}$–$\mathbf{TO_{30}}$) were determined to study the effects of the primary oligomer structure on binding and were compared with those of AB-type diblock oligomers ($\mathbf{DO_5}$–$\mathbf{DO_{50}}$). The binding efficiencies were 84% ($\mathbf{TO_5}$), 92% ($\mathbf{TO_{10}}$) and 40% ($\mathbf{TO_{30}}$), and that of $\mathbf{TO_{10}}$ was the highest among all block oligomers (Fig. 5, Table S2). Interestingly, all ABA-type triblock oligomers had higher binding affinities to the lipid membranes than did the AB-type diblock oligomers, even though each oligomer had the same hydrophobic BMA content. Indeed, $\mathbf{TO_5}$ bound to lipid membranes twice as efficiently as $\mathbf{DO_5}$, yet the BMA content in these oligomer chains was almost identical (BMA content = 16.7 mol%/oligomer). The length of the BMA segment was also important for stable binding to the lipid membranes: $\mathbf{TO_{10}}$ (BMA content = 28.6 mol%/oligomer) bound more efficiently to the membranes than did $\mathbf{TO_5}$, yet $\mathbf{DO_{10}}$ (BMA content = 28.6 mol%/oligomer) bound more effectively to the membranes than $\mathbf{DO_5}$. A plausible explanation for the significantly lower efficiency of $\mathbf{TO_{30}}$

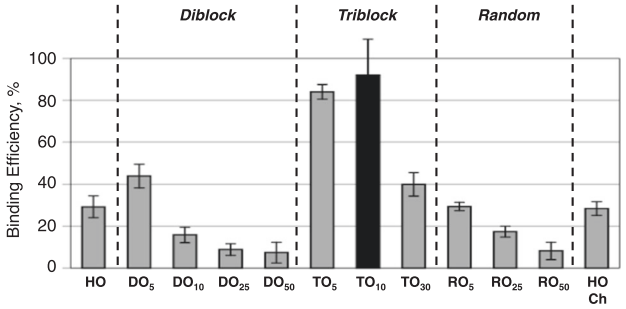

Fig. 5 Binding efficiency of amphiphilic oligomers to lipid membranes of liposome/silica, used as a model of cell membranes. Conditions: [oligomer]/[DOPC] = 1/10 (mol/mol) in HEPES buffer/methanol = 100/1 (v/v) at room temperature. The results are the means ± S.D.

was favorable micelle formation, as shown in Fig. 2, probably owing to the mismatch of the length of the BMA segments with the thickness of the DOPC bilayer (i.e., the BMA segment is longer than the membrane thickness). Therefore, suitable BMA content and segment length were necessary for the stable binding of oligomers as membrane anchors, and ABA-type triblock oligomers were more effective molecular devices than AB-type diblock oligomers.

Conclusions

A series of PEGylated amphiphilic block co-oligomers were prepared from PEGMA and BMA, via Ru-LRP, as a novel type of membrane anchor. Amphiphilic block oligomers were successfully bound to the lipid bilayer membranes of liposomes, which served as a cell model, with relatively high efficiencies of up to ~92% (**TO_{10}**), and no apparent cytotoxicity. The binding affinity to the membrane could be tuned by altering both the primary structure and the BMA content of the oligomers. Indeed, ABA-type triblock oligomers bound to lipid membranes more efficiently than did AB-type diblock and random oligomers. The length of the BMA segments and the BMA content in an oligomer were important factors determining its stable binding to membranes. Therefore, the amphiphilic block oligomers developed in our study could be useful as membrane anchors for related biomedical applications. Our oligomer conjugates could allow the control and diversification of functions on the cell surface, resulting in controlled cell recognition and cellular interactions for cell surface engineering. Furthermore, these proteoliposomes could contribute to the future development of tissue engineering and drug delivery systems. The currently available systems will also introduce new fields in cell surface engineering and contribute to the development of new biomedical applications, not only in tissue engineering but also in drug, protein, and RNA delivery.

Acknowledgements This work was supported by a Grant for Exploratory Research for Advanced Technology from the Japan Science and Technology Agency (JST-ERATO). This work was also supported by Grants-in-Aid from the Japan Society for the Promotion of Science (JSPS), KAKENHI grant numbers JP16H06313 (K.A.) and JP16H03842 (Y.S.). We thank Professor M. Sawamoto (Kyoto University) for support in performing the SEC analysis. We also thank S.R. Doctrow, PhD, from the Edanz Group (www.edanzediting.com/ac) for editing a draft of this manuscript.

Compliance with ethical standards

Conflict of interest The authors declare that they have no conflict of interest.

References

1. Custódio CA, Mano JF. Cell surface engineering to control cellular interactions. Chem Nano Mat. 2016;2:376–84.
2. Capicciotti CJ, Zong C, Sheikh MO, Sun T, Wells L, Boons G-J. Cell-surface glyco-engineering by exogenous enzymatic transfer using a bifunctional CMP-Neu5Ac derivative. J Am Chem Soc. 2017;139:13342–8.
3. Niu J, Lunn DJ, Pusuluri A, Yoo JI, Malley MAO, Mitragotri S, Soh HT, Hawker CJ. Engineering live cell surfaces with functional polymers via cytocompatible controlled radical polymerization. Nat Chem. 2017;9:537–45.
4. Mastuda M, Hatanaka W, Takeo M, Kim CW, Niidome T, Yamamoto T, Kishimura A, Mori T, Katayama Y. Short peptide motifs for long-lasting anchoring to the cell surface. Bioconjug Chem. 2014;25:2134–43.
5. Hoffecker IT, Takemoto N, Arima Y, Iwata H. Sequence-specific nuclease-mediated release of cells tethered by oligonucleotide phospholipids. Biomaterials. 2015;53:318–29.
6. Liu Q, Lyu Z, Yu Y, Zhao Z-A, Hu S, Yuan L, Chen G, Chen H. Synthetic glycopolymers for highly efficient differentiation of embryonic stem cells into neurons: lipo- or not? ACS Appl Mater. 2017;9:11518–27.
7. D'Souza S, Murata H, Jose MV, Askarova S, Yantsen Y, Andersen JD, Edington CDJ, Clafshenkel WP, Koepsel RR, Russell AJ. Engineering of cell membranes with a bisphosphonate-containing polymer using ATRP synthesis for bone targeting. Biomaterials. 2014;35:9447–58.
8. Muraoka T, Endo T, Tabata KV, Noji H, Nagatoishi S, Tsumoto K, Li R, Kinbara K. Reversible ion transportation switch by a ligand-gated synthetic supramolecular ion channel. J Am Chem Soc. 2014;136:15584–95.
9. Shi P, Ju E, Wang E, Yan Z, Ren J, Qu X. Host–guest recognition on photo-responsive cell surfaces directs cell–cell contacts. J Method. 2016;12:16–21.
10. Shi P, Ju E, Yan Z, Gao N, Wang J, Hou J, Zhang Y, Ren J, Qu X. Spatiotemporal control of cell–cell reversible interactions using molecular engineering. Nat Commun. 2016;7:1–9.
11. Langton MJ, Keymeulen F, Ciaccia M, Williams NH, Hunter CA. Controlled membrane translocation provides a mechanism for signal transduction and amplification. Nat Chem. 2017;9:426–30.
12. Lister FGA, Le Bailly BAF, Webb SJ, Clayden J. Ligand-modulated conformational switching in a fully synthetic membrane-bound receptor. Nat Chem. 2017;9:420–5.
13. Jia H-R, Wang H-Y, Yu Z-W, Chen Z, Wu F-G. Long-time plasma membrane imaging based on a two-step synergistic cell surface modification strategy. Bioconjug Chem. 2016;27:782–9.
14. Chen X, Zhang X, Wang H-Y, Chen Z, Wu F-G. Subcellular fate of a fluorescent cholesterol-poly(ethylene glycol) conjugate: an

excellent plasma membrane imaging reagent. Langmuir. 2016;32:10126–35.
15. Kobayashi S, Terai T, Yoshikawa Y, Ohkawa R, Ebihara M, Hayashi M, Takiguchi K, Nemoto N. In vitro selection of random peptides against artificial lipid bilayers: A potential tool to immobilize molecules on membranes. Chem Commun. 2017;53:3458–61.
16. Rosen BM, Percec V. Single-electron transfer and single-electron transfer degenerative chain transfer living radical polymerization. Chem Rev. 2009;109:5069–119.
17. Anastasaki A, Nikolaou V, Nurumbetov G, Wilson P, Kempe K, Quinn JF, Davis TP, Whittaker MR, Haddleton DM. Cu(0)-mediated living radical polymerization: a versatile tool for materials synthesis. Chem Rev. 2016;116:835–77.
18. Matyjaszewski K, Tsarevsky NV. Macromolecular engineering by atom transfer radical polymerization. J Am Chem Soc. 2014;136:6513–33.
19. Keddie DJ, Moad G, Rizzard E, Thang SH. RAFT agent design and synthesis. Macromolecules. 2012;45:5321–42.
20. Koda Y, Terashima T, Sawamoto M, Maynard HD. Amphiphilic/fluorous random copolymers as a new class of non-cytotoxic polymeric materials for protein conjugation. Polym Chem. 2015;6:240–7.
21. Koda Y, Terashima T, Maynard HD, Sawamoto M. Protein storage with perfluorinated PEG compartments in a hydrofluorocarbon solvent. Polym Chem. 2016;7:6694–8.
22. Pelegri-O'Day EM, Lin E-W, Maynard HD. Therapeutic protein-polymer conjugates: advancing beyond PEGylation. J Am Chem Soc. 2014;136:14323–32.
23. Nguyen TH, Kim S-H, Decker CG, Wong DY, Loo JA, Maynard HD. A heparin-mimicking polymer conjugate stabilizes basic fibroblast growth factor. Nat Chem. 2013;5:221–7.
24. Bat E, Lee J, Lau UY, Maynard HD. Trehalose glycopolymer resists allow direct writing of protein patterns by electron-beam lithography. Nat Commun. 2015;6:6654.
25. Lau UY, Saxer SS, Lee J, Bat E, Maynard HD. Direct write protein patterns for multiplexed cytokine detection from live cells using electron beam lithography. ACS Nano. 2016;10:723–9.
26. Delplace V, Nicolas J. Degradable vinyl polymers for biomedical applications. Nat Chem. 2015;7:771–84.
27. Boyer C, Corrigan NA, Jung K, Nguyen D, Nguyen T-K, Adnan NNM, Oliver S, Shanmugan S, Yeow J. Copper-mediated living radical polymerization (atom transfer radical polymerization and copper(0) mediated polymerization): from fundamentals to bioapplications. Chem Rev. 2016;116:1803–949.
28. Tu Y, Peng F, Adawy A, Men Y, Abdelmohsen LKEA, Wilson DA. Mimicking the cell: bio-inspired functions of supramolecular assemblies. Chem Rev. 2016;116:2023–78.
29. Palivan C, Goers R, Najer A, Zhang X, Car A, Meier W. Bioinspired polymer vesicles and membranes for biological and medical applications. Chem Soc Rev. 2016;45:377–411.
30. Ouchi M, Terashima T, Sawamoto M. Transition metal-catalyzed living radical polymerization: toward perfection in catalysis and precision polymer synthesis. Chem Rev. 2006;109:4963–5050.
31. Yoda H, Nakatani K, Terashima T, Ouchi M, Sawamoto M. Ethanol-mediated living radical homo- and copolymerizations with Cp*-ruthenium catalysts: active, robust, and universal for functionalized methacrylates. Macromolecules. 2010;43:5595–601.
32. Koda Y, Terashima T, Sawamoto M. Fluorous microgel star polymers: selective recognition and separation of polyfluorinated surfactants and compounds in water. J Am Chem Soc. 2014;136:15742–8.
33. Koda Y, Terashima T, Sawamoto M. Multimode self-folding polymers via reversible and thermoresponsive self-assembly of amphiphilic/fluorous random copolymers. Macromolecules. 2016;49:4534–43.
34. Weissig V. Liposomes. 2nd ed. In: Torchilin VP, editor. Oxford: Oxford Univ. Press; 2003.